Life Sciences 238 (2019) 116934

Contents lists available at ScienceDirect

Life Sciences

journal homepage: www.elsevier.com/locate/lifescie

Oroxylin A regulates the turnover of lipid droplet via downregulating adipose triglyceride lipase (ATGL) in hepatic stellate cells

Zili Zhang[a,1], Mei Guo[b,1], Min Shen[a,1], Yujia Li[a], Shanzhong Tan[c], Jiangjuan Shao[a,*], Feng Zhang[a], Anping Chen[d], Shijun Wang[e], Shizhong Zheng[a,**]

[a] Jiangsu Key Laboratory for Pharmacology and Safety Evaluation of Chinese Materia Medica, Nanjing University of Chinese Medicine, Nanjing, 210023, China
[b] Department of Pathogenic biology and Immunology, Medical School, Southeast University, Nanjing, 210009, China
[c] Nanjing Hospital Affiliated to Nanjing University of Chinese Medicine, Nanjing, 210023, China
[d] Department of Pathology, School of Medicine, Saint Louis University, St Louis, MO, 63104, USA
[e] Shandong co-innovation center of TCM formula, College of Traditional Chinese Medicine, Shandong University of Traditional Chinese Medicine, China

ARTICLE INFO

Keywords:
ATGL
Hepatic stellate cell
Lipid droplet
Oroxylin A
ROS

ABSTRACT

Proliferation and differentiation of hepatic stellate cells (HSCs) are the most noticeable events in hepatic fibrosis, in which the loss of lipid droplets (LDs) is the most important feature. However, the complex mechanisms of LD disappearance have not been fully elucidated. In the current study, we investigated whether oroxylin A has the pharmacological activity of reversing LDs in activated HSCs, and further examined its potential molecular mechanisms. Using genetic, pharmacological, and molecular biological measure, we found that LD content significantly decreased during HSC activation, whereas oroxylin A markedly reversed LD content in activated HSCs. Interestingly, oroxylin A treatment observably decreased the expression of adipose triglyceride lipase (ATGL) without large differences in classical LD synthesis pathway, LD-related transcription factors, and autophagy pathway. ATGL overexpression could completely impair the effect of oroxylin A on reversing LD content. Importantly, reactive oxygen species (ROS) signaling pathway mediated oroxylin A-induced ATGL downregulation and LD revision in activated HSCs. ROS specific stimulant buthionine sulfoximine (BSO) could dramatically diminish the antioxidant effect of oroxylin A, and in turn, abolish reversal effect of oroxylin A on LD content. Conversely, ROS specific scavenger N-acetyl cystenine (NAC) can significantly enhance the pharmacological effect of oroxylin A on LD revision. Taken together, our study reveals the important molecular mechanism of anti-fibrosis effect of oroxylin A, and also suggests that ROS-ATGL pathway is a potential target for reversing LDs.

1. Introduction

Hepatic fibrosis is a complex compensatory response, which is the only way for all chronic liver diseases to develop into cirrhosis [1–3]. If not diagnosed and detected in time, it will destroy normal liver structure and affect normal liver function, finally culminating in cirrhosis and hepatocellular carcinoma (HCC) [4–6]. It is universally agreed that proliferation and differentiation of hepatic stellate cells (HSCs) are the most noticeable events in hepatic fibrosis, in which the loss of lipid droplets (LDs) is the most important feature [7]. In normal physiological state, HSCs in normal liver contain large amounts of LDs in the cytoplasm, which is also the main reason why HSCs are called fat storage cells [8]. In abnormal pathological state, various injury factors stimulate HSCs to proliferate, in which HSCs lose their LDs and oversynthesize extracellular matrix (ECM) that triggers lesion in hepatic architecture [8]. Of note, it has been confirmed that the components of HSC LDs mainly include retinol, triglyceride and cholesterol [9]. Fatty acid is the metabolite of LDs, which can produce ATP by beta oxidation [10]. Many studies suggested that the loss of LDs is an important energy source for HSC activation [11–13]. Therefore, blocking LD metabolism could inhibit HSC activation by cutting off energy supply [14]. However, although LD disappearance of HSCs has attracted concerns of numerous scholars, the underlying molecular mechanisms are largely unknown.

It is well known that LD metabolism involves many signaling pathways including the classical LD synthesis pathway [15], LD

* Corresponding author. Nanjing University of Chinese Medicine, 138 Xianlin Avenue, Nanjing, Jiangsu, 210023, China.
** Corresponding author. Nanjing University of Chinese Medicine, 138 Xianlin Avenue, Nanjing, Jiangsu, 210023, China.
E-mail addresses: jjshao1976@163.com (J. Shao), nytws@163.com (S. Zheng).
[1] These authors contributed equally to this work.

https://doi.org/10.1016/j.lfs.2019.116934
Received 1 July 2019; Received in revised form 26 September 2019; Accepted 3 October 2019
Available online 11 October 2019
0024-3205/

degradation pathway [16], LD-related transcription factors [17], and recently discovered non-classical autophagy pathway [18]. The synthesis and degradation pathways of LDs are mainly involved in classical cytoplasmic short-term regulation, whereas LD-related transcription factors serve as an important role in long-term regulation in the nucleus [19]. Noteworthy, autophagy is a cellular protective mechanism against various extreme environments, which is closely related to various physiological and pathological processes [20]. However, it is used to be thought that autophagy is not selective for degradation of various intracellular components [21]. Until recently, scholars began to realize that the concept of autophagy was far beyond the cognitive of the past academic circles [22]. The recent discovery shows that autophagy represents a more selective process than originally expected, and that selective autophagy delivers a wide range of autophagic cargo [23]. Revealing molecular mechanism of LD disappearance will provide an innovative perspective for the diagnosis and prevention of hepatic fibrosis.

Oroxylin A ($C_{16}H_{12}O_5$), extracted from *Scutellaria baicalensis Georgi*, is a bioactive flavonoid [24]. Many studies supported that oroxylin A has a variety of pharmacological functions including anti-oxidant stress [25], anti-metastasis [26], anti-cell senescence [27], anti-hepatic steatosis [28], anti-inflammation [29], and so on. The evidence related to the current study is that oroxylin A can ameliorate hepatic fibrosis by inhibiting HSC activation [30–33]. Chen W et al. reported that induction of autophagy is necessary for oroxylin A to alleviate carbon tetrachloride-induced liver fibrosis and HSC activation [30]. Moreover, Zhang C et al. showed that the inhibition of YAP/HIF-1α signaling is required for oroxylin A to inhibit angiogenesis of liver sinusoidal endothelial cell (LSECs) in liver fibrosis [31]. Furthermore, Wang F et al. revealed that oroxylin A prevents HSC contraction by inhibiting dehydrogenase A dependent glycolysis [32]. Besides, Zhu R et al. revealed that treatment with oroxylin A accelerates liver regeneration in acute liver injury mice [33]. To our knowledge, few studies have assessed the effect of oroxylin A on LD turnover in activated HSCs.

In the current study, we found that oroxylin A can alleviate hepatic fibrosis by reversing LD content of activated HSCs. Further molecular mechanism studies showed that ROS-dependent adipose triglyceride lipase (ATGL) downregulation mediates oroxylin A-induced reversion of LDs. Our study provides experimental evidence for understanding of the important mechanisms of oroxylin A in anti-hepatic fibrosis.

2. Materials and methods

2.1. Antibodies and reagents

Recombinant mouse platelet derived growth factor-BB (PDGF-BB, #PMG0043), dimethyl sulfoxide (DMSO, #D12345), and N-acetyl-L-cysteine (NAC, #R210250) were obtained from Thermo Fisher Scientific (Waltham, MA, USA). Oroxylin A (#PHL82615), carbon tetrachloride (CCl_4, #488488), L-Buthionine-sulfoximine (BSO, #B2515), phosphate buffered saline (PBS, #P5368), and Dulbecco's Modified Eagle's Medium (DMEM, #D0819) were ordered from Sigma-Aldrich (St Louis, MO, USA). Trypsin-EDTA (#25200056), fetal bovine serum (FBS, #10099141), and Opti MEM medium (#31985062) were purchased from GIBCO BRL (Grand Island, NY, USA). Primary antibody against ATGL (#ab109251) was bought from Abcam (Cambridge, UK). Anti-mouse IgG (#7076) and anti-rabbit IgG (#7054) were purchased from Cell Signaling Technology (Danvers, MA, USA). SLC7A11 siRNA, control siRNA, ATGL plasmid, control vector, VA-Lip-ATGL-plasmid, and VA-Lip-Control-vector were obtained from Hanbio (Shanghai, China). Lipofectamine™ 3000 Transfection Reagent (#L3000008) was ordered from Thermo Fisher Scientific (Waltham, MA, USA).

2.2. Establishment of animal model and drug treatment scheme

Male C57BL/6 mice were ordered from Nanjing Medical University (Nanjing, China) at the age of about 8 weeks. Fifty mice were randomly divided into five groups on average. According to previous reports [34–36], 10% CCl_4 solution (0.5 ml/100 g bodyweight) was used to establish classical mouse liver fibrosis model. Briefly, mice from control group were intraperitoneally (i.p.) injected with olive oil of equal volume as a negative control. Mice from CCl_4 + VA-Lip-Control-vector group were i.p. injected with CCl_4 (every other day for 8 weeks) and were injected with VA-Lip-Control-vector by tail vein (every two weeks for 8 weeks). Mice from CCl_4 + VA-Lip-Control-vector + oroxylin A group were i.p. injected with CCl_4 (every other day for 8 weeks), injected with VA-Lip-Control-vector by tail vein (every two weeks for 8 weeks), and were treated with oroxylin A (20 mg/kg, every day from the last four weeks). Mice from CCl_4 + VA-Lip-ATGL-plasmid group were i.p. injected with CCl_4 (every other day for 8 weeks) and were injected with VA-Lip-ATGL-plasmid by tail vein (every two weeks for 8 weeks). Mice from CCl_4 + VA-Lip-ATGL-plasmid + oroxylin A group were i.p. injected with CCl_4 (every other day for 8 weeks), injected with VA-Lip-ATGL-plasmid by tail vein (every two weeks for 8 weeks), and were treated with oroxylin A (20 mg/kg, every day from the last four weeks). After the experiment, all liver samples were collected completely. All experimental procedures were approved by the institutional and local committee on the care and use of animals of Nanjing University of Chinese Medicine (Nanjing, China), and all animals received humane care according to the National Institutes of Health (USA) guidelines.

2.3. Histopathological examination

The obtained liver tissue samples were treated with 10% stationary solution (#G6257, Sigma-Aldrich) for 2 days. Then, the liver tissue was dehydrated in 70% ethanol for 5 min, 95% ethanol for 5 min two times, 100% ethanol for 15 min three times. Subsequently, these tissue sections were embedded in molten paraffin and catted into 5-μm thick slices. The sections were stained with hematoxylin and eosin (H&E) staining, masson staining, and sirius red staining for pathological examination.

2.4. Isolation and culture of primary HSCs

Primary mouse HSCs were isolated from normal male C57BL/6 mice according to previous literature reports [34–36]. Isolated HSCs were cultured in cell culture medium including 90% DMEM, 10% FBS, and 1% antibiotics, and were maintained at 37 °C in a humidified atmosphere of 5% CO_2 and 95% air.

2.5. Plasmid construction and gene transfection

ATGL plasmid and control vector were used to increase ATGL expression in vitro, while VA-Lip-ATGL-plasmid and VA-Lip-Control-vector were used to upregulate ATGL expression in vivo according to the reported method [34–36]. Real-time PCR was used to further validate the transfection efficiency.

2.6. Detection of LD content by nile red staining

The LD content of HSCs was determined by Nile red staining according to previous reports [36]. Briefly, a proper amount of HSCs were treated with indicated treatments, and then were immobilized with paraformaldehyde (#16005, Sigma-Aldrich) for 15 min, and were stained with Nile red in different concentrations of isopropanol (#278475, Sigma-Aldrich). HSCs were washed with PBS for 5 min, and the typical images of LDs were captured by inverted microscope with 100 amplification.

Table 1
Primer sequences.

Gene	Forward	Reverse
α-SMA	5′-GCCACATCGCTCAGACACC-3′	5′-CCCAATACGACCAAATCCGT-3′
Collagen1	5′-CGATGGCGTGCTATGCAA-3′	5′-ACTCGCCCTCCCGTTTTT-3′
Fibronectin	5′-GGGCAAGTTTCCAGGTACAG-3′	5′-CAGCTCTGCAGT GTCGTCTT-3′
Desmin	5′-AGCTCAAGTCATCGCCCTTC-3′	5′-GCAGATCCCAACACCCTCTC-3′
FAS	5′-CAAATACAATGGCACCCTGA-3′	5′-TGGCGAAGCCGTAGTTAGTT-3′
ACC	5′-TACTGAACTACATCTTCTCCC-3′	5′-AAGCAATAAGAACCTGACGA-3′
DGAT1	5′-TTCCGCCTCTGGGCATT-3′	5′-AGAATCGGCCCACAATCCA-3′
DGAT2	5′-AGTGGCAATGCTATCATCATCGT-3′	5′-TCTTCTGGACCCATCGGCCCCAGGA-3′
ACSL3	5′-CAATTACAGAAGTGTGGGACT-3′	5′-CACCTTCCTCCCAGTTCTTT-3′
ACAT1	5′-AGCCCAGAAAAATTTCATGGACACATACAG-3′	5′-CCCTTGTTCTGGAGGTGCTCTCAGATCTTT-3′
ACAT2	5′-TTTGCTCTATGCCTGCTTCA-3′	5′-CCATGAAGAGAAAGGTCCACA-3′
MGAT1	5′-CTGGTTCTGTTTCCCGTTGT-3′	5′-TGGGTCAAGGCCATCTTAAC-3′
HMG-CoA	5′-CAGGATGCAGCACAGAATGT-3′	5′-CTTTGCATGCTCCTTGAACA-3′
HSL	5′-GCCACAATGACACAGTCACTGGT-3′	5′-CAGGCAGCGGCCGTAGAAGCA-3′
ATGL	5′-GAGACCAAGTGGAACATC-3′	5′-GTAGATGTGAGTGGCGTT-3′
HL	5′-GCCTTTCTCCTGATGACGCT-3′	5′-AACTCAGGCAGAGCCCTTTC-3′
LPL	5′-CGAGAGGATCCGAGTGAAAG-3′	5′-TTTGTCCAGTGTCAGCCAGA-3′
PPARα	5′-CCTCAGGGTACCACTACGGAGT-3′	5′-GCCGAATAGTTCGCCGAA-3′
PPARγ	5′-TTTCAAGGGTGCCAGTTT-3′	5′-GAGGCCAGCATCGTGTAG-3′
SREBP-1C	5′-GTGAGCCTGACAAGCAATCA-3′	5′-GGTGCCTACAGAGCAAGAGG-3′
C/EBP-α	5′-CAAGAACAGCAACGAGTACCG-3′	5′-GTCACTGGTCAACTCCAGCAC-3′
NRF2	5′-AGGACATGGAGCAAGTTTGG-3′	5′-AGGACATGGAGCAAGTTTGG-3′
LC3	5′-ATCATCGAGCGCTACAAGGGTGA-3′	5′-GGATGATCTTGACCAACTCGCTCAT-3′
ATG3	5′-TGATGGGGGATGGGTAGATA-3′	5′-GCTTCCCCTTCATCTTCCTC-3′
ATG5	5′-GTGCTTCGAGATGTGTGGTTTGGA-3′	5′-CGTCAAATAGCTGACTCTTGGCAA-3′
BECN1	5′-AGGTACCGACTTGTTCCCTA-3′	5′-TCCATCCTGTACGGA AGACA-3′
ATG7	5′-GCTAATGGACACCAGGGAGA-3′	5′-AAAAAGTGAGGAGCCCAGGT-3′
ATG9	5′-GTGCTTATTGCCCTCACCAT-3′	5′-GGCATGTAGTGGATGTGTGC-3′
ATG12	5′-ACAAAGAAATGGGCTGTGGA-3′	5′-TTTGCAGTAATGCAGGACCA-3′
ATG14	5′-CTAGACCACCCCTATCGTGA-3′	5′-CCACAATCTCACAAGGCTGA-3′
P62	5′-GTGGGACAGCCAGAGGAACA-3′	5′-GCCCTTCCGATTCTGGCAT-3′
SLC7A11	5′-TTGCAAGCTCACAGCAATTCTG-3′	5′-CAGGTCCAGACGCAGGATGGC-3′
SLC3A2	5′-CCAGAATGCCGAGATGATAGA-3′	5′-CACTTGAGGCCAAGAGTTGA-3′
GAPDH	5′-GCCACATCGCTCAGACACC-3′	5′-CCCAATACGACCAAATCCGT-3′

2.7. Detection of main components and products of LDs

The levels of retinol (#YFXER00573, YIFEIXUE BIO TECH), cholesterol (#MAK043-1 KT, Sigma), triglycerides (#TRI19-1 KT, Sigma), and fatty acid (#MAK044, Sigma) were determined by commercially available kits according to manufacturer's instructions [36].

2.8. Real-time PCR analysis

After the appropriate amount of HSCs was treated with indicated treatments, the total RNA was completely extracted using the RNA extraction kit (#DP419, TIANGEN). cDNA synthesis was conducted using TransScript First-Strand cDNA Synthesis SuperMix (#AT301-02, TransGen Biotech). qRT-PCR was performed using TransStart Green qPCR SuperMix (#AQ101-01, TransGen Biotech). Primer sequences were present in Table 1.

2.9. Western blot analysis

HSC cells were washed three times with PBS and then used for extraction of total proteins. Protein extracts were prepared by mammalian lysis buffer (#MCL1, Sigma-Aldrich). Protein concentration was measured using BCA Protein Quantification Kit (#P0006, Beyotime). 40 μg/well proteins were separated by SDS-polyacrylamide gel (#M00652, GenScript), and then were transferred to a PVDF membrane (#88518, Thermo Fisher Scientific). The membranes were blocked with Western Blocking Buffer (#SW3010, Solarbio), and then were incubated overnight at 4 °C with the primary antibody against ATGL (#ab109251, 1/1000 dilution, Abcam). Next, the membranes were incubated with a secondary antibody (#7054, 1/10000 dilution, Cell Signaling Technology) for 1 h at room temperature. Protein bands were visualized using the chemiluminescence system (Merck Millipore, Darmstadt, Germany). Densitometry analysis was performed using Image J software.

2.10. Detection of intracellular ROS level

After the appropriate amount of HSCs was treated with indicated treatments, intracellular ROS levels were measured using Reactive oxygen species assay kit (#CA1410, Solarbio) according to manufacturer's instructions [36].

2.11. Detection of intracellular GSH level

After the appropriate amount of HSCs was treated with indicated treatments, intracellular GSH levels were measured using Reduced glutathione assay kit (#A006-2, Nanjing Jiancheng Bioengineering Institute) according to manufacturer's instructions [36].

2.12. Transmission electron microscopy

After the appropriate amount of HSCs was treated with indicated treatments, cell climbing tablets was fixed by glutaraldehyde for 15 min. Classic LD images were collected using transmission electron microscope (#EM208S, Olympus) [34–36].

2.13. Statistical analyses

Data were expressed as mean ± standard error of the mean (SEM). Statistical analysis was performed using either Student's t-test (two-group comparison) or one-way analysis of variance followed by Student-Newman-Keuls test (more than two groups). In all analyses, a probability of less than 0.05 was considered to indicate statistical significance. All statistical analyses were performed using the SPSS

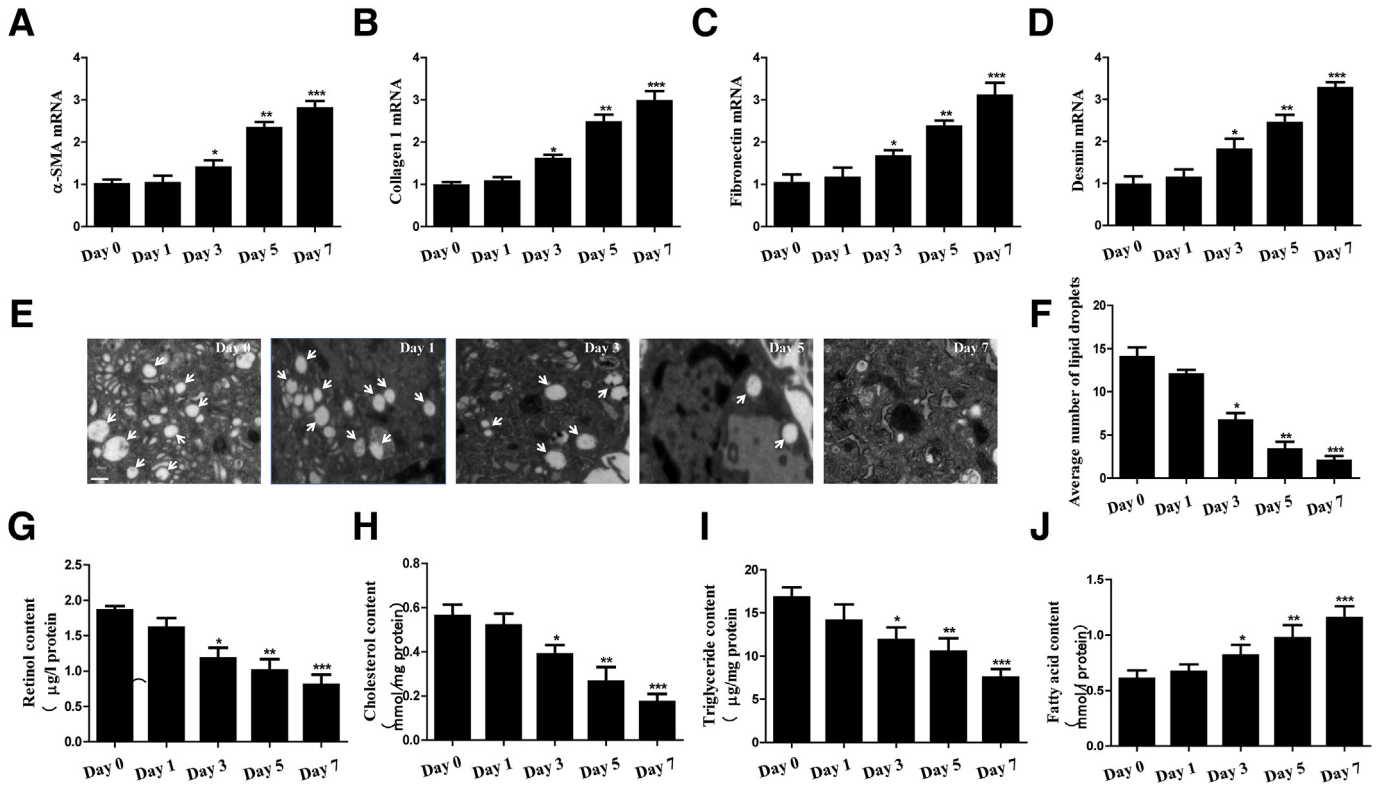

Fig. 1. LD content significantly decreased during HSC activation.

program (version 20.0; IBM, Somers, NY, USA).

3. Results

3.1. LD content significantly decreased during HSC activation

Many important studies suggested that in vitro stimulation of PDGF-BB can lead to the activation of quiescent primary HSCs, which may simulate HSC activation in vivo during hepatic fibrosis [9,37]. Therefore, quiescent primary mouse HSCs, which were isolated from normal C57BL/6 mice [38], were treated with PDGF-BB for 7 days. As expected, we found that the expression level of HSC activation markers including α-SMA (Fig. 1A), collagen1 (Fig. 1B), fibronectin (Fig. 1C), and desmin (Fig. 1D) was increased almost 3 fold, when HSCs were treated with PDGF-BB for 7 days. These results were in good agreement with the previous theoretical and experimental studies that treatment with PDGF-BB triggered the activation of HSCs in vitro [9,37]. Meanwhile, we also detected the content of LDs from quiescent HSCs (Day 0) to activated HSCs (Day 7). Interestingly, the most intuitive detection method transmission electron microscope (TEM) showed that numerous LDs present in the cytoplasm of quiescent HSCs (Day 0), whereas few LDs appeared in the cytoplasm of activated HSCs (Day 7) (Fig. 1E). Similarly, quantitative statistical analysis of the number of LDs revealed that the number of LDs decreased by 50%, 80% and 90% respectively, after 3, 5 and 7 days of PDGF-BB treatment (Fig. 1F). Importantly, it is well known that retinol, triglyceride and cholesterol are the main constituents of LDs [39]. Therefore, we determined the content of retinol, triglyceride and cholesterol during HSC activation. Interestingly, with the activation of HSCs, the level of retinol (Fig. 1G), cholesterol (Fig. 1H) and triglyceride (Fig. 1I) was all significantly decreased. Of note, fatty acids are the main degradation products of LD metabolism, and can provide energy for the activation of HSC by producing ATP through oxidation [40]. Indeed, compared with quiescent HSCs (Day 0), the fatty acid content of activated HSCs (Day 7) almost increased by 2 folds (Fig. 1J). Overall, these results indicated that LD content significantly decreased during HSC activation.

3.2. Oroxylin A markedly reversed LD content in activated HSCs

Numerous studies have confirmed that oroxylin A can inhibit HSC activation [30–33], but the complex mechanisms have not been fully elucidated. In the current study, we hypothesized that oroxylin A inhibits HSC activation by restoring LD phenotype. To verify this hypothesis, quiescent primary HSCs were treated with PDGF-BB for 7 days, following treatment with different concentrations of oroxylin A for 24 h. Interestingly, Nile red staining showed that treatment with PDGF-BB evidently reduced LD content compared with control, whereas oroxylin A treatment increased LD content in a dose-dependent manner (Fig. 2A). Moreover, we also measured the contents of three important components of LDs. As expected, treatment with oroxylin A completely eliminated PDGF-BB-induced reduction of retinol (Fig. 2B), cholesterol (Fig. 2C) and triglyceride (Fig. 2D). It is important to note that high-doses of oroxylin A almost restored the lipid content of activated HSCs to quiescent state (Fig. 2A–D). Furthermore, the metabolites of LDs were also detected following oroxylin A treatment. Attractively, fatty acid content significantly increased during HSC activation, suggesting that fatty acid storage sites LDs markedly reduced (Fig. 2E). By contrast, oroxylin A treatment remarkably impaired PDGF-BB-driven fatty acid upregulation (Fig. 2E). Meanwhile, we further determined the inhibitory function of oroxylin A on HSC activation. Real-time PCR showed that oroxylin A treatment down-regulated the expression of HSC activation markers α-SMA (Fig. 2F), collagen1 (Fig. 2G), fibronectin (Fig. 2H), and desmin (Fig. 2I). Altogether, these findings suggest that oroxylin A markedly reversed LD content in activated HSCs.

3.3. The downregulation of ATGL was required for oroxylin A to reverse LD content in activated HSCs

To further investigate the molecular mechanism of oroxylin A-

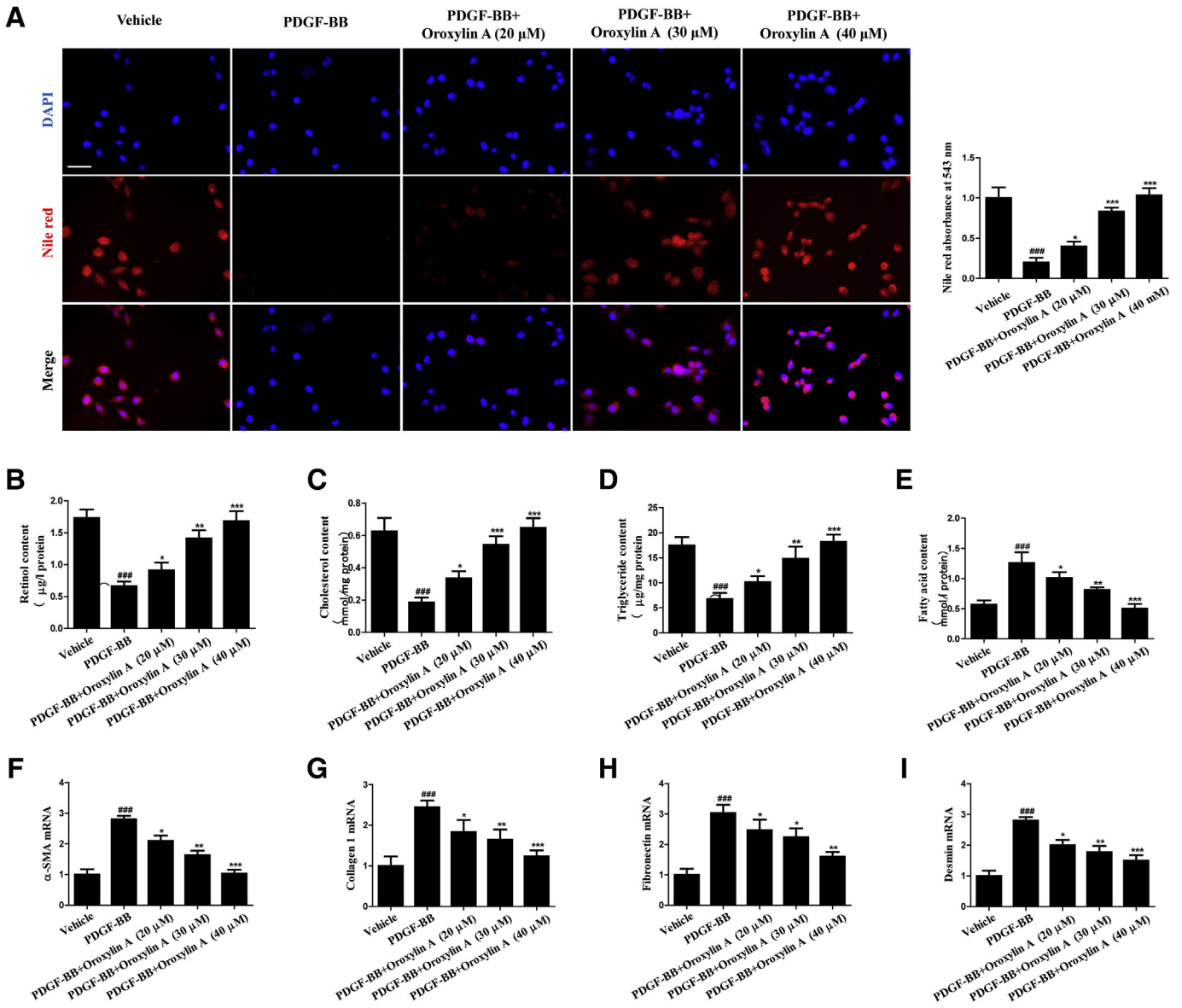

Fig. 2. Oroxylin A markedly reversed LD content in activated HSCs.

induced LD reversal, we investigated changes of the classical LD synthesis pathway (Fig. 3A), LD degradation pathway (Fig. 3B), LD-related transcription factors (Fig. 3D), and non-classical autophagy pathway (Fig. 3C) in activated HSCs. Interestingly, real-time PCR showed that treatment with oroxylin A observably reduced the expression of ATGL without large differences in classical LD synthesis pathway, LD-related transcription factors, and autophagy pathway, although the expression of hormone-sensitive lipase (HSL) and autophagy-related gene 5 (ATG5) was slightly changed (Fig. 3A–D). Furthermore, western blot also confirmed that oroxylin A treatment reduced the protein expression of ATGL in a dose-dependent manner (Fig. 3E). These data suggest that oroxylin A-induced LD reversal was probably based on the inhibition of ATGL in the classical LD degradation pathway. To further validate this hypothesis, we constructed an ATGL overexpression plasmid for reverse validation. Of note, ATGL plasmid not only increased the expression of ATGL by about 2.5 folds, but also completely counteracted the oroxylin A-induced ATGL downregulation (Fig. 3F). Subsequently, we examined the effect of ATGL plasmid on LD content. As expected, ATGL overexpression could reduce intracellular lipid content, and also significantly decreased oroxylin A-mediated increase of intracellular lipid (Fig. 3G), suggesting involvement of ATGL in the reversion of intracellular LDs. Besides, oroxylin A treatment almost doubled the diameter of LDs, whereas ATGL plasmid partially eliminated the promotion of oroxylin A (Fig. 3H). Additionally, we examined the effect of oroxylin A combined with ATGL plasmid on the main components of LDs. Similarly, treatment with oroxylin A alone significantly increased retinol (Fig. 3I), cholesterol (Fig. 3J) and triglyceride (Fig. 3K) levels, but the combination of oroxylin A and ATGL plasmid did not evidently increase their levels (Fig. 3I–K). It is well-known that fatty acids are the main degradation products of LD metabolism, and can provide energy for the activation of HSC by producing ATP through oxidation [40]. Therefore, we determined the effect of oroxylin A on fatty acid level. Interestingly, oroxylin A treatment dramatically reduced fatty acid levels, whereas ATGL overexpression almost impaired the inhibitory action of oroxylin A (Fig. 3L). More importantly, we explored whether overexpression of ATGL could impair the effect of oroxylin A on HSC activation. Attractively, ATGL plasmid completely reduced the inhibitory effect of oroxylin A on HSC activation markers α-SMA (Fig. 3M), collagen1 (Fig. 3N), fibronectin (Fig. 3O), and desmin (Fig. 3P). Collectively, these findings support the hypothesis that the downregulation of ATGL was required for oroxylin A to reverse LD content in activated HSCs.

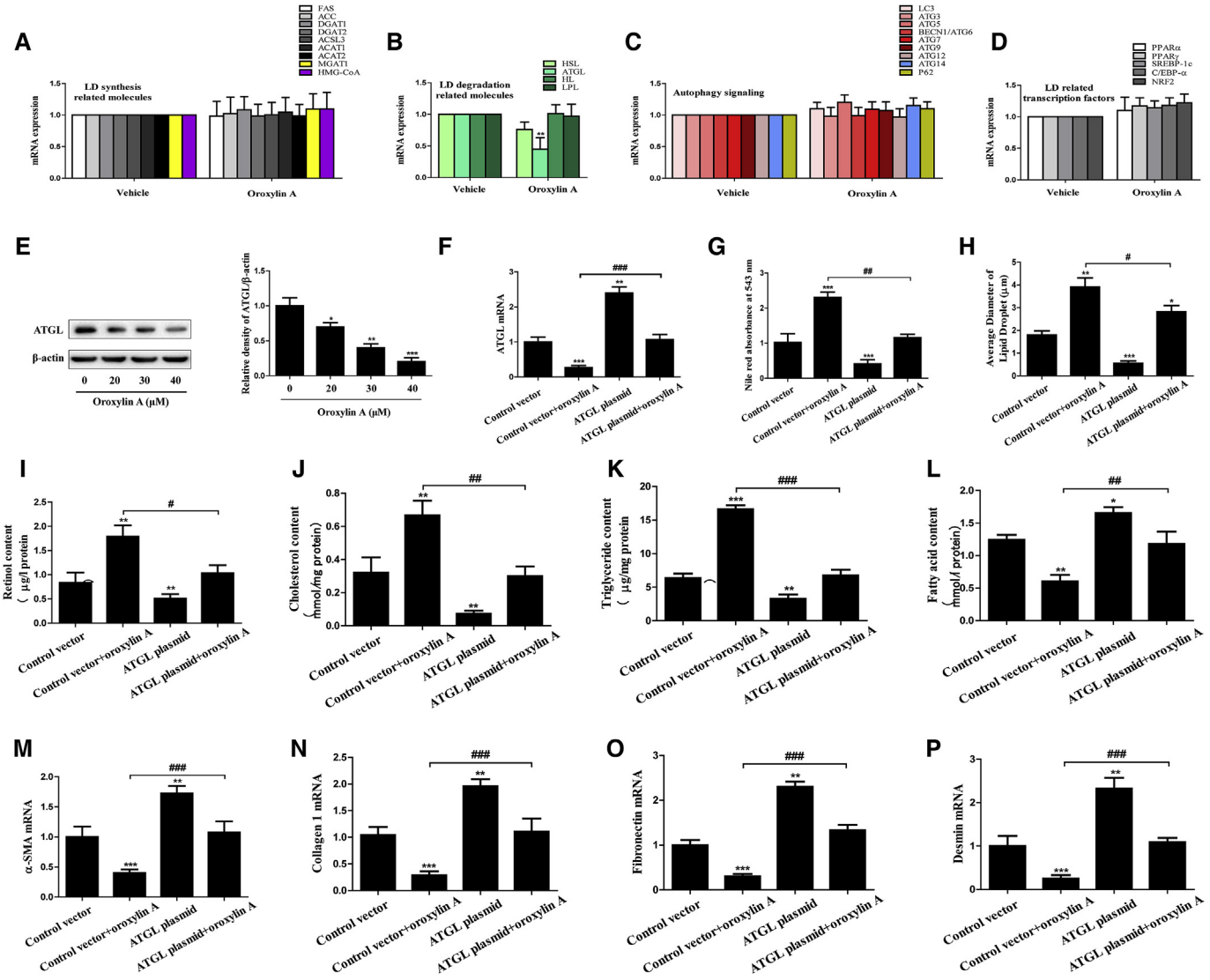

Fig. 3. The downregulation of ATGL was required for oroxylin A to reverse lipid droplet content in activated HSCs. (A–D) Quiescent primary HSCs were exposed to 20 ng/ml PDGF-BB for 7 days, and then were treated with 20 μM oroxylin A for 24 h. The mRNA expression of the LD synthesis, degradation, transcription factors, and autophagy related molecules was determined by real-time PCR analysis. **(E)** Quiescent primary HSCs were exposed to 20 ng/ml PDGF-BB for 7 days, and then were treated with different concentrations of oroxylin A (20, 30, 40 μM) for 24 h. The protein expression of ATGL was examined by western blot analysis. **(F)** Quiescent primary HSCs stably transfected with ATGL plasmid were exposed to 20 ng/ml PDGF-BB for 7 days, and then were treated with 20 μM oroxylin A for 24 h. The mRNA expression of ATGL was determined by real-time PCR analysis. **(G, H)** LD content was examined by Nile red staining, and average diameter of LDs was measured. **(I–L)** The levels of retinol, cholesterol, triglycerides, and fatty acid were determined by commercially available kits. **(M–P)** The mRNA expression of α-SMA, collagen 1, fibronectin, and desmin was determined by real-time PCR analysis. For the statistics of each panel in this figure, data are expressed as mean ± SD (n = 3). *P < 0.05 versus Control vector, **P < 0.01 versus Control vector, ***P < 0.001 versus Control vector. $^{\#}$P < 0.05 versus Control vector + oroxylin A, $^{\#\#}$P < 0.01 versus Control vector + oroxylin A, $^{\#\#\#}$P < 0.001 versus Control vector + oroxylin A. . (For interpretation of the references to colour in this figure legend, the reader is referred to the Web version of this article.)

3.4. ROS signaling pathway mediated oroxylin A-induced ATGL downregulation and LD reversal in activated HSCs

A large number of studies have pointed out that oxidative stress is closely related to LD metabolism [41,42]. Therefore, we assumed that ROS metabolic system may be involved in the reversal of LDs and the downregulation of ATGL induced by oroxylin A. To test this assumption, we first examined the levels of ROS and GSH during LD disappearance. In line with many previous studies [43–45], ROS level increased and GSH level decreased with the reduction of LD content (Fig. 4A). These findings suggest that the ROS accumulation may drive the loss of LDs during HSC activation. Subsequently, we explored the effects of oroxylin A on intracellular ROS and GSH levels. Interestingly, treatment with oroxylin A dose-dependently reduced ROS accumulation and increased GSH content (Fig. 4B) in activated HSCs. Importantly, under elevated ROS conditions, endogenous L-Cysteine production is insufficient for GSH synthesis, and the system X_c^--mediated uptake of exogenous cystine is required for the production of L-Cysteine and subsequent synthesis of GSH [46]. Therefore, we hypothesized that oroxylin A reduced ROS levels and increased GSH levels in a system X_c^--dependent mechanism. To test this hypothesis, we determined the effect of oroxylin A on system X_c^- (SLC7A11/SLC3A2). Interestingly, oroxylin A treatment significantly upregulated the expression of SLC7A11, but did not markedly affect the expression of SLC3A2 (Fig. 4C). More importantly, siRNA-mediated knockdown of SLC7A11 completely impaired oroxylin A-induced SLC7A11 upregulation (Fig. 4D), and, in turn, abolished oroxylin A-induced ROS reduction and GSH generation (Fig. 4D). To further confirm the role of ROS in

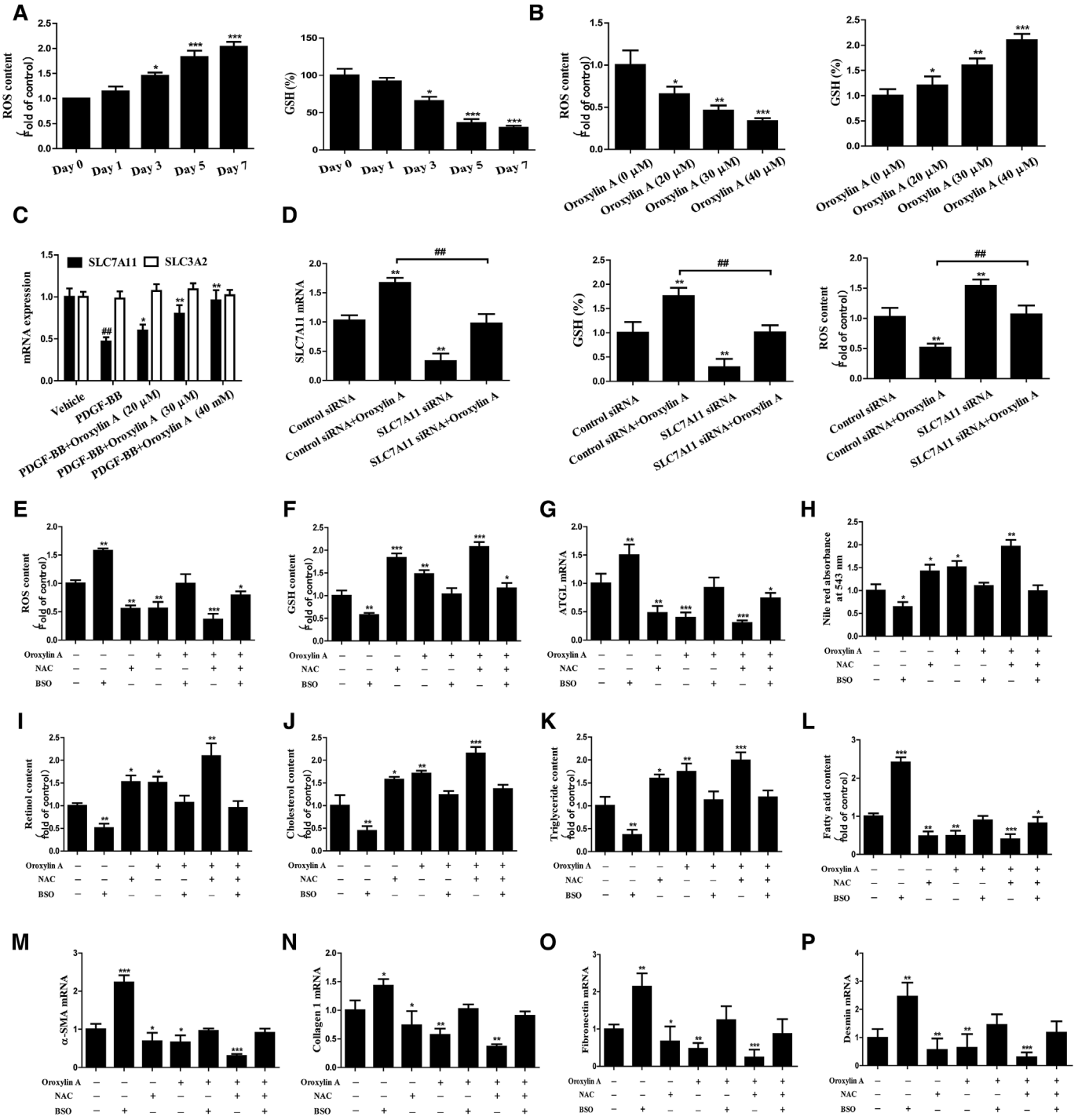

Fig. 4. ROS signaling pathway mediated oroxylin A-induced ATGL downregulation and LD reversal in activated HSCs. **(A)** Quiescent primary HSCs were exposed to 20 ng/ml PDGF-BB for 7 days. The levels of ROS and GSH were determined. **(B)** Quiescent primary HSCs were exposed to 20 ng/ml PDGF-BB for 7 days, and then were treated with different concentrations of oroxylin A (20, 30, 40 μM) for 24 h. The levels of ROS and GSH were determined. **(C)** The expression of SLC7A11 and SLC3A2 was determined by real-time PCR analysis. **(D)** Quiescent primary HSCs stably transfected with SLC7A11 siRNA were exposed to 20 ng/ml PDGF-BB for 7 days, and then were treated with 20 μM oroxylin A for 24 h. The expression of SLC7A11 and the levels of ROS and GSH were determined. **(E, F)** Quiescent primary HSCs were exposed to 20 ng/ml PDGF-BB for 7 days, and then were treated with 20 μM oroxylin A or 10 mM NAC or 5 mM BSO for 24 h. The levels of ROS and GSH were determined. **(G)** The mRNA expression of ATGL was determined by real-time PCR analysis. **(H)** LD content was examined by Nile red staining. **(I–L)** The levels of retinol, cholesterol, triglycerides, and fatty acid were determined by commercially available kits. **(M–P)** The mRNA expression of α-SMA, collagen 1, fibronectin, and desmin was determined by real-time PCR analysis. For the statistics of each panel in this figure, data are expressed as mean ± SD (n = 3). *P < 0.05 versus Control, **P < 0.01 versus Control, ***P < 0.001 versus Control.

the reversal of LDs induced by oroxylin A, the levels of cellular ROS and GSH were altered by either NAC, a precursor of GSH by supplying cysteine, or by BSO, a specific inhibitor of glutamate-cysteine ligase. As expected, oroxylin A as well as NAC markedly eliminated ROS accumulation (Fig. 4E) and increased the levels of cellular GSH (Fig. 4F). However, the pretreatment of cells with BSO not only remarkably driven ROS accumulation and depleted cellular GSH levels, but also diminished the antioxidant effect of oroxylin A or NAC (Fig. 4E

and F). Next, we further explore the regulatory effect of ROS on ATGL in oroxylin A-treated cells. Attractively, NAC-induced ROS scavenge was able to enhance the inhibitory effect of oroxylin A on ATGL (Fig. 4G), whereas pretreatment with BSO impaired oroxylin A-induced ATGL downregulation (Fig. 4G). Furthermore, the LD content and its degradation product were all detected. Importantly, ROS clearance induced by NAC enhanced the reversal of LDs by oroxylin A (Fig. 4H-L), but ROS accumulation induced by BSO weakened the effect of oroxylin A on LD reversion (Fig. 4H-L). In addition, we also examined the effect of ROS on the inhibition of HSC activation by oroxylin A. ROS removal by NAC or oroxylin A could downregulate the expression of HSC activation markers α-SMA (Fig. 4M), collagen1 (Fig. 4N), fibronectin (Fig. 4O), and desmin (Fig. 4P), whereas ROS accumulation by BSO could upregulate their expression (Fig. 4M–P). Altogether, ROS scavenging mediated oroxylin A-induced ATGL downregulation and LD reversal in activated HSCs.

3.5. Oroxylin A reversed LD content in an ATGL-dependent mechanism in vivo

In order to study the potential mechanism of oroxylin A-induced LD reversion in vivo, we used VA-Lip-ATGL-plasmid to target upregulate ATGL expression in activated HSCs [35]. First of all, the effect of VA-Lip-ATGL-plasmid on liver fibrosis was examined by macroscopic examination. As shown in Fig. 5A, the classical fibrosis changes occurred in the liver of model mice compared with the control, but oroxylin A treatment significantly alleviated the pathological state of liver fibrosis. Interestingly, VA-Lip-ATGL-plasmid not only aggravated liver fibrosis, but also partially counteracted the anti-fibrosis effect of oroxylin A (Fig. 5A). Moreover, pathological analysis was used to detect collagen deposition in fibrotic scar area [36]. As expected, treatment with oroxylin A reduced collagen deposition, whereas VA-Lip-ATGL-plasmid almost eliminated the pharmacological effects of oroxylin A (Fig. 5B). More importantly, primary HSCs were further isolated to detect LD content. Of note, oroxylin A treatment increased the levels of LDs (Fig. 5C), retinol (Fig. 5D), cholesterol (Fig. 5E) and triglyceride (Fig. 5F), whereas VA-Lip-ATGL-plasmid apparently abolished pharmacological activity of oroxylin A (Fig. 5C–F). Furthermore, the levels of ROS and GSH in primary HSCs were determined. Attractively, oroxylin A exhibited significant antioxidant activity, but VA-Lip-ATGL-plasmid abolished its effects (Fig. 5G and H). Additionally, the influence of VA-Lip-ATGL-plasmid on HSC activation markers was detected. Consistently, treatment with oroxylin A reduced the expression of HSC activation markers α-SMA (Fig. 5I) and collagen1 (Fig. 5J), whereas pretreatment with VA-Lip-ATGL-plasmid impaired anti-hepatic fibrosis effect of oroxylin A (Fig. 5I and J). Overall, oroxylin A reversed LD content in an ATGL-dependent mechanism in vivo.

4. Discussion

Hepatic fibrosis is a complex chronic pathological process, and activation of HSCs has been considered as the most important fibrosis-promoting event [7]. Attractively, among the numerous morphological and biochemical changes in HSC activation, the loss of LDs is the most noticeable phenomenon [8]. The most important discovery at present is that LD loss is mainly used to provide sufficient energy for sustained activation of HSCs [11–13]. Therefore, blocking the disappearance of LDs and cutting off the energy supply may become a new strategy to inhibit the activation of HSCs. Recently, Qiu S et al. showed that the blockade of lipophagy pathway is necessary for docosahexaenoic acid to regulate LD turnover of activated HSCs, and to inhibit HSC activation [47]. Moreover, Miyamae Y et al. demonstrated that tetrandrine induces lipid accumulation through blockade of autophagy in a hepatic stellate cell line, which is a potential mechanism of anti-hepatic fibrosis [48]. Furthermore, Lin J et al. revealed that perilipin 5 restores the formation of LDs in activated HSCs and inhibits HSC activation [49]. In addition, Zhang F et al. found that curcumin raises lipid content by Wnt pathway to inhibit HSC activation [50]. Consistent with previous literature reports, we showed that LD reversion of activated HSCs effectively improved the pathological conditions of the hepatic fibrosis in the classical animal model. Meanwhile, we also identified and characterized a novel mechanism of oroxylin A-induced LD revision of activated HSCs in hepatic fibrosis. Oroxylin A markedly reversed LD content in activated HSCs, which depends on ATGL downregulation. To our knowledge, although many literatures have reported that oroxylin A has excellent anti-hepatic fibrosis pharmacological activity [30–33], few researches studied the molecular mechanism of oroxylin A's anti-fibrosis from the perspective of LD reversal. Our study is the first to point out that restoring LD phenotype of activated HSCs may be a potential molecular mechanism of oroxylin A's anti-hepatic fibrosis effect.

As an almost universal rule, the homeostasis of LDs is regulated synthetically by both the classical lipolysis pathway and recently discovered non-classical autophagy pathway [15–18]. Interestingly, to further explore the molecular mechanism of oroxylin A-induced LD reversal, we investigated changes of the classical LD synthesis pathway, LD degradation pathway, LD-related transcription factors, and autophagy pathway in activated HSCs, following oroxylin A treatment. Importantly, oroxylin A treatment observably decreased the expression of ATGL without large differences in classical LD synthesis pathway, LD-related transcription factors, and autophagy pathway, although the expression of HSL and ATG5 was slightly changed. These results suggest that oroxylin A-induced LD reversal was probably based on the inhibition of ATGL in the classical LD degradation pathway. These results fixed our attention to the classical pathway of lipolysis in the following study of molecular mechanism. Although our results suggest that the mechanism of LD reversal is related to classical lipolysis, we cannot rule out that other potential mechanisms also play an important role. Hernández-Gea V et al. showed that autophagy releases lipid that promotes fibrogenesis in mice and in human tissues [51]. Moreover, Zhang Z et al. also found that autophagy regulates turnover of LDs via ROS-dependent Rab25 activation in activated HSCs [9]. Additionally, Yokomori H et al. reported that Caveolin-1 is related to LD formation in HSCs [52]. Caveolin-1 transport to LDs might represent an intracellular pathway from the endoplasmic reticulum in cirrhotic liver tissue [52]. Chen M et al. revealed that AMP-activated protein kinase regulates lipid metabolism and the fibrotic phenotype of HSCs through inhibition of autophagy [53]. In addition, Lin J et al. demonstrated that perilipin 5 restores the formation of LDs in activated HSCs and inhibits HSC activation [49]. It may be that each drug has its own unique molecular mechanism. The characteristic of oroxylin A is that it regulates classical lipolysis pathway rather than autophagy pathway. The origin of this characteristic may be attributed to the drug structure of oroxylin A.

ATGL functions as a key enzyme catalyzing the conversion of triacylglycerol stores to fatty acid during intracellular lipolysis [54]. Therefore, regulation of ATGL activity is important for maintaining dynamic balance of LD storage and metabolism [54]. Interestingly, Schweiger M et al. reported that pharmacological inhibition of ATGL corrects high-fat diet-induced insulin resistance and hepatosteatosis in mice [55]. Moreover, Grace SA et al. showed that ATGL expression is associated with adiposity and tumor stromal proliferation in patients with pancreatic ductal adenocarcinoma [56]. Furthermore, Riederer M et al. demonstrated that downregulation of ATGL reduces arachidonic acid release and prostacyclin secretion in human aortic endothelial cells [57]. Besides, Chen G et al. revealed that lncRNA SRA induces hepatic steatosis through inhibiting the expression of ATGL [58]. Importantly, in the current study, we found that the downregulation of ATGL was required for oroxylin A to reverse LD content in activated HSCs. Treatment with oroxylin A reduced the protein expression of ATGL in a dose-dependent manner. Meanwhile, ATGL overexpression could reduce intracellular lipid content, and also significantly decreased oroxylin A-mediated increase of intracellular lipid, strongly suggesting involvement of ATGL in the reversion of intracellular LDs. Although our

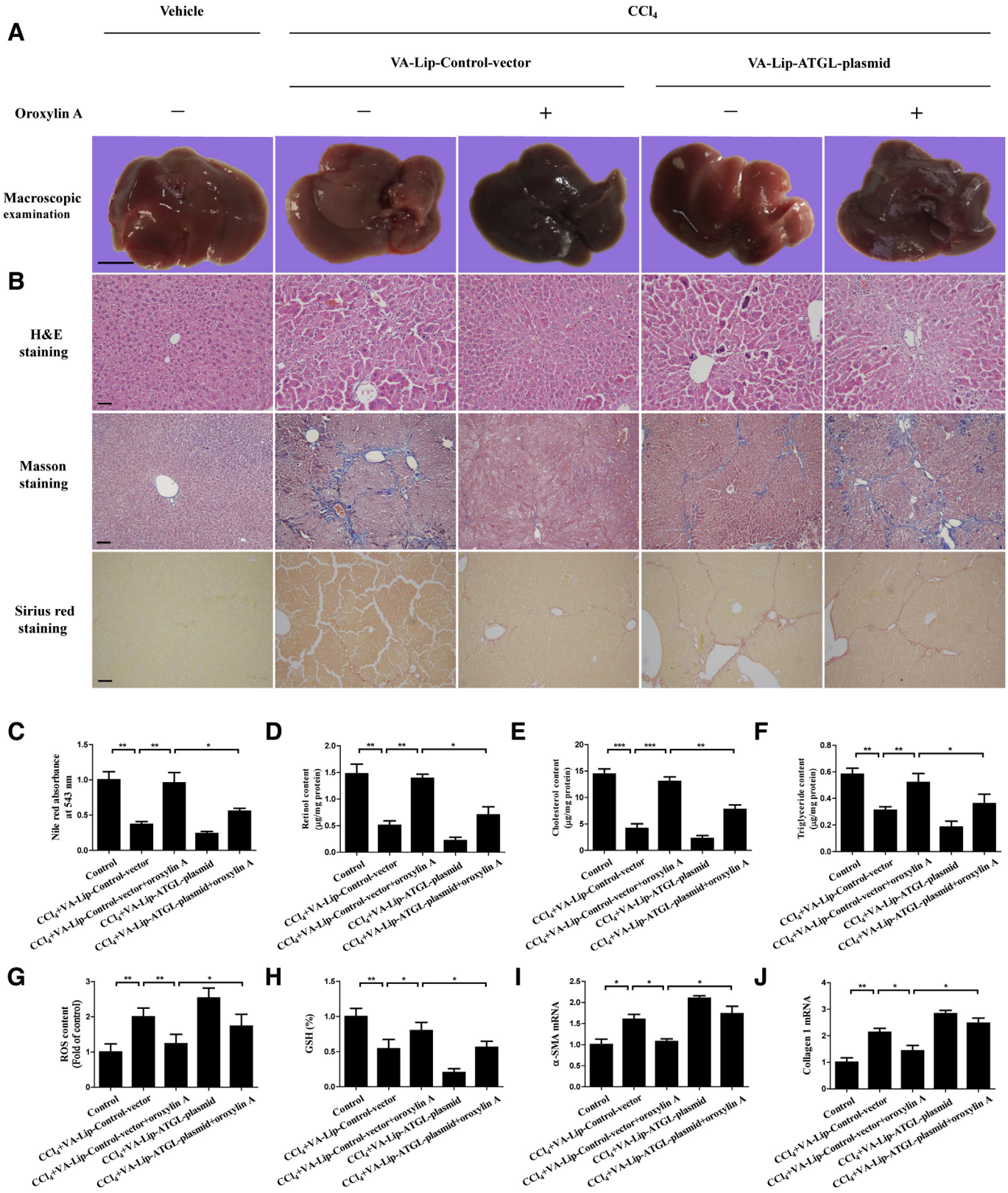

Fig. 5. Oroxylin A reversed LD content in an ATGL-dependent mechanism in vivo.
Fifty male C57BL/6 mice were treated with vehicle, CCl_4 + VA-Lip + Control vector, CCl_4 + VA-Lip + Control vector + Oroxylin A, CCl_4 + VA-Lip + ATGL plasmid, and CCl_4 + VA-Lip + ATGL plasmid + Oroxylin A. **(A)** Morphological changes of the liver were examined by macroscopic examination. The representative pictures were showed, and the Bar is 1 cm. **(B)** Collagen deposition in fibrotic scar area was detected by pathological analysis. The representative pictures were showed, and the Bar is 50 μm. **(C)** Primary HSCs were isolated, and LD content was examined by Nile red staining. **(D–F)** The levels of retinol, cholesterol, and triglycerides were determined by commercially available kits. **(G, H)** The levels of ROS and GSH were determined. **(I, J)** The mRNA expression of α-SMA and collagen 1 was determined by real-time PCR analysis. For the statistics of each panel in this figure, data are expressed as mean ± SD (n = 6). *P < 0.05, **P < 0.01, ***P < 0.001. . (For interpretation of the references to colour in this figure legend, the reader is referred to the Web version of this article.)

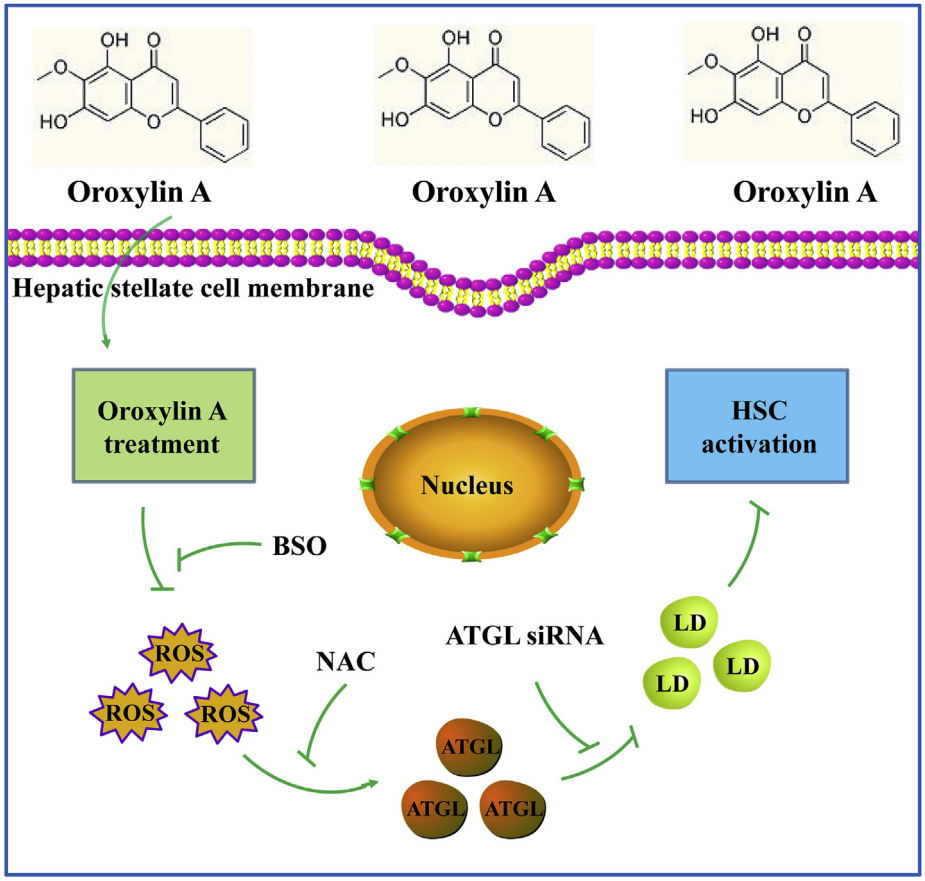

Fig. 6. Oroxylin A regulates the turnover of LD via downregulating ATGL in hepatic stellate cellsOroxylin A induces reversion of LDs by depressing ROS-dependent ATGL in activated HSCs, which can inhibit HSC activation and alleviate hepatic fibrosis.

research reveals the key role of ATGL in the reversal of LDs by oroxylin A, we do not know why oroxylin A has the most significant regulatory effect on ATGL than other molecules. An acceptable hypothesis is that the chemical structure of oroxylin A has a higher affinity with the molecular structure of ATGL, but this hypothesis needs further experimental verification. Another concern is that oroxylin A can increase LD content in HSC cytoplasm by inhibiting ATGL, and whether oroxylin A can also increase LD levels in other cell types? It requires more experiments to verify. Nevertheless, our study is the first to reveal the important role of ATGL in the pharmacological activity of oroxylin A against hepatic fibrosis.

The close relationship between oxidative stress and lipid metabolism has been confirmed by many literatures [41,42]. Recently, Pang XY et al. showed that retinol saturase modulates lipid metabolism and the production of ROS [59]. Similarly, Pereira HA et al. reported that fluoride intensifies hypercaloric diet-induced endoplasmic reticulum oxidative stress and alters lipid metabolism [60]. Moreover, Pan YX et al. found that oxidative stress and mitochondrial dysfunction mediated Cd-induced hepatic lipid accumulation in zebrafish Danio rerio [61]. Additionally, Lee J et al. demonstrated that oxidative stress triggers LD accumulation in primary cultured hepatocytes by activating fatty acid synthesis [62]. More importantly, Yilancioglu K et al. identified oxidative stress as a mediator for increased lipid accumulation in a newly isolated dunaliella salina strain [63]. Considering the above research background, we proposed hypothesis that ROS metabolic system may be involved in the reversal of LDs and the downregulation of ATGL induced by oroxylin A. To test this assumption, we first examined the levels of ROS and GSH during LD disappearance. In line with many previous studies, ROS level increased and GSH level decreased with the reduction of LD content. These findings suggest that the accumulation of ROS may drive the loss of LDs during HSC activation. Subsequently, we explored the effects of oroxylin A on intracellular ROS and GSH levels. Interestingly, treatment with oroxylin A dose-dependently reduced ROS accumulation and increased GSH content in activated HSCs. Attractively, ROS clearance induced by NAC observably enhanced the reversal of LDs by oroxylin A, but ROS accumulation induced by BSO weakened the effect of oroxylin A on LD reversion. Of note, NAC-induced ROS scavenge was able to significantly enhance the inhibitory effect of oroxylin A on ATGL, whereas pretreatment with BSO prominently impaired oroxylin A-induced ATGL downregulation. Our study reveals the potential molecular mechanisms underlying oroxylin A regulation of ATGL and reversal of LDs.

Our study has several limitations that should be mentioned. First, this study lacks the support of clinical data. The results obtained from this study need to be verified in a multicenter study with a large sample size. Second, this study was only performed in primary mouse HSCs, and more HSC cell lines such as HSC-T6 (rat HSC lines) and HSC-LX2 (human HSC lines) need to be used to validate the results. Third, we used VA-Lip-ATGL-plasmid to target upregulate ATGL expression of HSCs in vivo. However, the transfection efficiency is not high, and more reliable transgenic mice should be used for experimental verification.

5. Conclusion

In summary, we found that oroxylin A induces reversion of LDs by depressing ROS-dependent ATGL in activated HSCs (Fig. 6). These findings are especially noteworthy because they provide an experimental basis for the development of oroxylin A as a novel anti-hepatic fibrosis drug and identify ATGL as a potential target for screening drugs for lipid metabolism diseases.

Declaration of competing interest

The authors declare no competing or financial interests.

Acknowledgments

This work also was supported by the National Natural Science Foundation of China (31571455, 31600653, 81870423 and 81600483), the Open Project Program of Jiangsu Key Laboratory for Pharmacology and Safety Evaluation of Chinese Materia Medica (No. JKLPSE 201804), the Project of the Priority Academic Program Development of Jiangsu Higher Education Institutions, the Youth Natural Science Foundation of Jiangsu Province (BK20140955), the Natural Science Research General Program of Jiangsu Higher Education Institutions (14KJB310011), the Youth Natural Science Foundation of Nanjing University of Chinese Medicine (13XZR20).

References

[1] B.S. Ding, Z. Cao, R. Lis, et al., Divergent angiocrine signals from vascular niche balance liver regeneration and fibrosis, Nature 505 (2014) 97–102.
[2] C.D. De Magalhaes Filho, M. Downes, R. Evans, Bile acid analog intercepts liver fibrosis, Cell 166 (2016) 789.
[3] Y. Chang, Y.K. Cho, Y. Kim, et al., Nonheavy drinking and worsening of noninvasive fibrosis markers in nonalcoholic fatty liver disease: a cohort study, Hepatology 69 (2019) 64–75.
[4] P. Rawla, T. Sunkara, P. Muralidharan, et al., Update in global trends and aetiology of hepatocellular carcinoma, Contemp. Oncol. 22 (2018) 141–150.
[5] C. Lackner, D. Tiniakos, Fibrosis and alcohol-related liver disease, J. Hepatol. 70 (2019) 294–304.
[6] E. Vilar-Gomez, L. Calzadilla-Bertot, V. Wai-Sun Wong, et al., Fibrosis severity as a determinant of cause-specific mortality in patients with advanced nonalcoholic fatty liver disease: a multi-national cohort study, Gastroenterology 155 (2018) 443–457.
[7] C.R. Gandhi, Hepatic stellate cell activation and pro-fibrogenic signals, J. Hepatol. 67 (2017) 1104–1105.
[8] N.A. Shackel, M.A. Vadas, J.R. Gamble, et al., Beyond liver fibrosis: hepatic stellate cell senescence links obesity to liver cancer by way of the microbiome, Hepatology 59 (2014) 2413–2415.
[9] Z. Zhang, S. Zhao, Z. Yao, et al., Autophagy regulates turnover of lipid droplets via ROS-dependent Rab25 activation in hepatic stellate cell, Redox Biol 11 (2017) 322–334.
[10] W.S. Blaner, S.M. O'Byrne, N. Wongsiriroj, et al., Hepatic stellate cell lipid droplets: a specialized lipid droplet for retinoid storage, Biochim. Biophys. Acta 1791 (2009) 467–473.
[11] S. Qiu, H. Xu, Z. Lin, et al., The blockade of lipophagy pathway is necessary for docosahexaenoic acid to regulate lipid droplet turnover in hepatic stellate cells, Biomed. Pharmacother. 109 (2019) 1841–1850.
[12] M. Pawlak, P. Lefebvre, B. Staels, Molecular mechanism of PPARα action and its impact on lipid metabolism, inflammation and fibrosis in non-alcoholic fatty liver disease, J. Hepatol. 62 (2015) 720–733.
[13] X. Cheng, Q. Sun, RUBCNL/Pacer and RUBCN/Rubicon in regulation of autolysosome formation and lipid metabolism, Autophagy 15 (2019) 1120–1121.
[14] M. Chen, J. Liu, W. Yang, et al., Lipopolysaccharide mediates hepatic stellate cell activation by regulating autophagy and retinoic acid signaling, Autophagy 13 (2017) 1813–1827.
[15] Y. Li, W.X. Zong, W.X. Ding, Recycling the danger via lipid droplet biogenesis after autophagy, Autophagy 13 (2017) 1995–1997.
[16] K.T. Nguyen, C.S. Lee, S.H. Mun, et al., N-terminal acetylation and the N-end rule pathway control degradation of the lipid droplet protein PLIN2, J. Biol. Chem. 294 (2019) 379–388.
[17] X. Xu, J.G. Park, J.S. So, et al., Transcriptional activation of Fsp27 by the liver-enriched transcription factor CREBH promotes lipid droplet growth and hepatic steatosis, Hepatology 61 (2015) 857–869.
[18] K.W. Chung, K.M. Kim, Y.J. Choi, et al., The critical role played by endotoxin-induced liver autophagy in the maintenance of lipid metabolism during sepsis, Autophagy 13 (2017) 1113–1129.
[19] F. Wilfling, J.T. Haas, T.C. Walther, et al., Lipid droplet biogenesis, Curr. Opin. Cell Biol. 29 (2014) 39–45.
[20] T.B. Nguyen, J.A. Olzmann, Lipid droplets and lipotoxicity during autophagy, Autophagy 13 (2017) 2002–2003.
[21] S. Takáts, S. Tóth, G. Szenci, et al., Investigating non-selective autophagy in drosophila, Methods Mol. Biol. 1880 (2019) 589–600.
[22] L. Yu, Y. Chen, S.A. Tooze, Autophagy pathway: cellular and molecular mechanisms, Autophagy 14 (2018) 207–215.
[23] T. Kimura, A. Jain, S.W. Choi, et al., TRIM-directed selective autophagy regulates immune activation, Autophagy 13 (2017) 989–990.
[24] H.B. Li, F. Chen, Isolation and purification of baicalein, wogonin and oroxylin A from the medicinal plant Scutellaria baicalensis by high-speed counter-current chromatography, J. Chromatogr. A 1074 (2005) 107–110.
[25] Q. Han, H. Wang, C. Xiao, et al., Oroxylin A inhibits H_2O_2-induced oxidative stress in PC12 cells, Nat. Prod. Res. 31 (2017) 1339–1342.
[26] W.T. Ku, J.J. Tung, T.J. Lee, et al., Long-term exposure to Oroxylin A inhibits metastasis by suppressing CCL2 in oral squamous cell carcinoma cells, Cancers 11 (2019) 1–6.
[27] H. Jin, N. Lian, M. Bian, et al., Oroxylin A inhibits ethanol-induced hepatocyte senescence via YAP pathway, Cell Prolif 51 (2018) e12431.
[28] H. Jin, N. Lian, M. Bian, et al., Oroxylin A prevents alcohol-induced hepatic steatosis through inhibition of hypoxia inducible factor 1alpha, Chem. Biol. Interact. 285 (2018) 14–20.
[29] W. Zhou, X. Liu, X. Zhang, et al., Oroxylin A inhibits colitis by inactivating NLRP3 inflammasome, Oncotarget 8 (2017) 58903–58917.
[30] W. Chen, Z. Zhang, Z. Yao, et al., Activation of autophagy is required for Oroxylin A to alleviate carbon tetrachloride-induced liver fibrosis and hepatic stellate cell activation, Int. Immunopharmacol. 56 (2018) 148–155.
[31] C. Zhang, M. Bian, X. Chen, et al., Oroxylin A prevents angiogenesis of LSECs in liver fibrosis via inhibition of YAP/HIF-1α signaling, J. Cell. Biochem. 119 (2018) 2258–2268.
[32] F. Wang, Y. Jia, M. Li, et al., Blockade of glycolysis-dependent contraction by oroxylin a via inhibition of lactate dehydrogenase-a in hepatic stellate cells, Cell Commun. Signal. 17 (2019) 11.
[33] R. Zhu, G. Zeng, Y. Chen, et al., Oroxylin A accelerates liver regeneration in CCl_4-induced acute liver injury mice, PLoS One 8 (2013) e71612.
[34] Y. Jia, F. Wang, Q. Guo, et al., Curcumol induces RIPK1/RIPK3 complex-dependent necroptosis via JNK1/2-ROS signaling in hepatic stellate cells, Redox Biol 19 (2018) 375–387.
[35] Z. Zhang, Z. Yao, L. Wang, et al., Activation of ferritinophagy is required for the RNA-binding protein ELAVL1/HuR to regulate ferroptosis in hepatic stellate cells, Autophagy 14 (2018) 2083–2103.
[36] Z. Zhang, Z. Yao, S. Zhao, et al., Interaction between autophagy and senescence is required for dihydroartemisinin to alleviate liver fibrosis, Cell Death Dis. 8 (2017) e2886.
[37] S.L. Zhang, L. Ma, J. Zhao, et al., The phenylethanol glycoside liposome inhibits PDGF-induced HSC activation via regulation of the FAK/PI3K/AKT signaling pathway, Molecules 24 (2019) 18.
[38] S. Weiskirchen, C.G. Tag, S. Sauer-Lehnen, et al., Isolation and culture of primary murine hepatic stellate cells, Methods Mol. Biol. 1627 (2017) 165–191.
[39] H. Senoo, Y. Mezaki, M. Fujiwara, The stellate cell system (vitamin A-storing cell system), Anat. Sci. Int. 92 (2017) 387–455.
[40] V. Hernández-Gea, S.L. Friedman, Autophagy fuels tissue fibrogenesis, Autophagy 8 (2012) 849–850.
[41] J. Lee, T. Homma, T. Kurahashi, et al., Oxidative stress triggers lipid droplet accumulation in primary cultured hepatocytes by activating fatty acid synthesis, Biochem. Biophys. Res. Commun. 464 (2015) 229–235.
[42] M.S. Krishna, B. Joy, A. Sundaresan, Effect on oxidative stress, glucose uptake level and lipid droplet content by Apigenin 7, 4'-dimethyl ether isolated from Piper longum L, J. Food Sci. Technol. 52 (2015) 3561–3570.
[43] Z. Tian, Y. Chen, N. Yao, et al., Role of mitophagy regulation by ROS in hepatic stellate cells during acute liver failure, Am. J. Physiol. Gastrointest. Liver Physiol. 315 (2018) 374–384.
[44] Z. Zhang, M. Guo, S. Zhao, et al., ROS-JNK1/2-dependent activation of autophagy is required for the induction of anti-inflammatory effect of dihydroartemisinin in liver fibrosis, Free Radic. Biol. Med. 101 (2016) 272–283.
[45] A. Galli, G. Svegliati-Baroni, E. Ceni, et al., Oxidative stress stimulates proliferation and invasiveness of hepatic stellate cells via a MMP2-mediated mechanism, Hepatology 41 (2005) 1074–1084.
[46] T. Demuyser, L. Deneyer, E. Bentea, et al., SLC7A11 (xCT) protein expression is not altered in the depressed brain and system X_c^- deficiency does not affect depression-associated behaviour in the corticosterone mouse model, World J. Biol. Psychiatry 20 (2019) 381–392.
[47] S. Qiu, H. Xu, Z. Lin, et al., The blockade of lipophagy pathway is necessary for docosahexaenoic acid to regulate lipid droplet turnover in hepatic stellate cells, Biomed. Pharmacother. 109 (2019) 1841–1850.
[48] Y. Miyamae, Y. Nishito, N. Nakai, et al., Tetrandrine induces lipid accumulation through blockade of autophagy in a hepatic stellate cell line, Biochem. Biophys. Res. Commun. 477 (2016) 40–46.
[49] J. Lin, A. Chen, Perilipin 5 restores the formation of lipid droplets in activated hepatic stellate cells and inhibits their activation, Lab. Investig. 96 (2016) 791–806.
[50] F. Zhang, C. Lu, W. Xu, et al., Curcumin raises lipid content by Wnt pathway in hepatic stellate cell, J. Surg. Res. 200 (2016) 460–466.
[51] V. Hernández-Gea, Z. Ghiassi-Nejad, R. Rozenfeld, et al., Autophagy releases lipid that promotes fibrogenesis by activated hepatic stellate cells in mice and in human tissues, Gastroenterology 142 (2012) 938–946.
[52] H. Yokomori, W. Ando, M. Oda, Caveolin-1 is related to lipid droplet formation in hepatic stellate cells in human liver, Acta Histochem. 121 (2019) 113–118.
[53] M. Chen, J. Liu, L. Yang, et al., AMP-activated protein kinase regulates lipid metabolism and the fibrotic phenotype of hepatic stellate cells through inhibition of autophagy, FEBS Open Bio 7 (2017) 811–820.
[54] I.K. Cerk, L. Wechselberger, M. Oberer, Adipose triglyceride lipase regulation: an overview, Curr. Protein Pept. Sci. 19 (2018) 221–233.
[55] M. Schweiger, M. Romauch, R. Schreiber, et al., Pharmacological inhibition of adipose triglyceride lipase corrects high-fat diet-induced insulin resistance and hepatosteatosis in mice, Nat. Commun. 8 (2017) 14859.
[56] S.A. Grace, M.W. Meeks, Y. Chen, et al., Adipose triglyceride lipase (ATGL) expression is associated with adiposity and tumor stromal proliferation in patients with pancreatic ductal adenocarcinoma, Anticancer Res. 37 (2017) 699–703.

[57] M. Riederer, M. Lechleitner, H. Köfeler, et al., Reduced expression of adipose triglyceride lipase decreases arachidonic acid release and prostacyclin secretion in human aortic endothelial cells, Arch. Physiol. Biochem. 123 (2017) 249–253.
[58] G. Chen, D. Yu, X. Nian, et al., LncRNA SRA promotes hepatic steatosis through repressing the expression of adipose triglyceride lipase (ATGL), Sci. Rep. 6 (2016) 35531.
[59] X.Y. Pang, S. Wang, M.J. Jurczak, et al., Retinol saturase modulates lipid metabolism and the production of reactive oxygen species, Arch. Biochem. Biophys. 633 (2017) 93–102.
[60] H.A. Pereira, A.S. Dionizio, M.S. Fernandes, et al., Fluoride intensifies hypercaloric diet-induced ER oxidative stress and alters lipid metabolism, PLoS One 11 (2016) e0158121.
[61] Y.X. Pan, Z. Luo, M.Q. Zhuo, et al., Oxidative stress and mitochondrial dysfunction mediated Cd-induced hepatic lipid accumulation in zebrafish Danio rerio, Aquat. Toxicol. 199 (2018) 12–20.
[62] J. Lee, T. Homma, T. Kurahashi, et al., Oxidative stress triggers lipid droplet accumulation in primary cultured hepatocytes by activating fatty acid synthesis, Biochem. Biophys. Res. Commun. 464 (2015) 229–235.
[63] K. Yilancioglu, M. Cokol, I. Pastirmaci, et al., Oxidative stress is a mediator for increased lipid accumulation in a newly isolated Dunaliella salina strain, PLoS One 9 (2014) e91957.